ISSN:2089 – 0133 Indonesian Journal of Applied Physics (2015) Vol.5 No.1 Halaman55
April 2015

# Photoluminescence Emission and StructureStudy in ZnO:Ag nanorods

**E. Velázquez-Lozada[1,*], G. M. Camacho-González[2], J. M. Quino-Cerdan[3]**

[1]SEPI – ESIME – Instituto Politécnico Nacional, Col. Lindavista, México D.F. C.P. 07738, México.
[2]ESIME – Instituto Politécnico Nacional, Col. Lindavista, México D.F. C.P. 07738, México.
[3]Universidad Tecnológica de México. Campus Atizapán. Edo. México. México.
[*] evlozada5@yahoo.com.mx

Received 1-11-2014, Revised 5-02-2015, Accepted 11-02-2015, Published 30-04-2015

## ABSTRACT

Scanning electronic microscopy (SEM) and X ray diffraction (XRD) have been applied to the study of structural and optical properties of ZnO nanocrystals prepared by the ultrasonic spray pyrolysis (USP) at different temperatures. The variation of temperatures and times at the growth of ZnO films permits modifying the ZnO phase from the amorphous to crystalline, to change the size of ZnO nanocrystals (NCs), as well as to vary their photoluminescence spectra.

*Keywords:*Nanorods, ZnO:Ag, XRD, Photoluminescence

## INTRODUCTION

Nanocrystalline Zinc oxide (ZnO) with wide band gap energy nearly 3.37 eV, high exciton binding energy (60 meV at 300K) and easy way of nanostructure preparation has attracted great attention during the last two decades [1]. In addition to exceptional exciton properties, ZnO possesses a number of deep levels that emit in the whole visible range and, hence, can provide intrinsic "white" light emission. ZnO nanostructures are being investigated as promising candidates for different optoelectronic applications, such as: the non-linear optical devices [2], light-emitting devices [3-6], transparent electrodes for solar cells [7] and laser diodes [8], as well as for the excellent field emitters [9], electrochemical sensors and toxic gas sensors [10]. The control of the ZnO defect structure in these nanostructures is a necessary step in order to improve the device quality. Since the structural imperfection and defects generally deteriorate the exciton related recombination process, it is necessary to grow the high quality films for efficient light-emitting applications. The ultrasonic spray pyrolysis (USP) method offers many advantages such as easy compositional modifications; easy introducing the various functional groups, relatively low annealing temperatures and the possibility of coating deposition on a large area substrate. It will be interesting to study the optical emission of USP produced ZnO NCs doped by Ag in order to identify the best regimes for obtaining the bright emitting nanosystems. The motivation of Ag doping on ZnO that should be added in Nanostructures is because of a range of complementary techniques was used to explore the physical mechanisms of Ag doping in ZnO and in this work, we have PL, XRD and SEM study and have understanding of property types that have to use Ag as a dopant.

## SAMPLES AND EXPERIMENTAL DETAILS

ZnO:Ag thin solid films were prepared by the USP technique (Fig. 1) on the surface of soda-lime glass substrate for the two substrate temperatures (400 and 450 $^0$C) and different deposition times (Table 1).

**Table 1.** Technological regimes and NC parameters from SEM images

| Sample numbers | Growth temperature (°C) | Deposition time (min) | NR width (nm) |
|---|---|---|---|
| 1 | 400 | 10 | 150-200 |
| 2 | 400 | 5 | 100-150 |
| 3 | 400 | 3 | 50-70 |
| 4 | 450 | 10 | 200-250 |
| 5 | 450 | 5 | 120-180 |
| 6 | 450 | 3 | 80-110 |

The deposition system presented in figure 1 includes a piezoelectric transducer operating at variable frequencies up to 1.2 MHz and the ultrasonic power of 120 W. ZnO:Ag thin solid films were deposited from a 0.4 M solution of zinc (II) acetate [Zn(O2CCH3)2] (Alfa), dissolved in a mix of deionized water, acetic acid [CH3CO2H] (Baker), and methanol [CH3OH] (Baker) (100:100:800 volume proportion).Separately, a 0.2 M solution of silver nitrate [Ag($NO_3$)] (Baker) dissolved in a mix of deionized water and acetic acid [$CH_3CO_2H$] (Baker) (1:1 volume proportion) was prepared, in order to be used as doping source. A constant [Ag]/[Zn] ratio of 2 at. % was applied at the ZnO Ag film preparation.

The morphology of ZnO:Ag films has been studied by secondary electrons signals using the scanning electron microscopy (SEM) Dual Beam, FEI brand, model Quanta 3D FEG with field emission gun. PL spectra were at the excitation by a He-Cd laser with a wavelength of 325 nm and a beam power of 20 mW at 300K using a PL setup on a base of spectrometer SPEX500 described in [11, 12]. The crystal structure of ZnO:Ag films was investigated by the X-ray diffraction (XRD) using the diffractometer Model XPERT MRD with the Pixel detector, three axis goniometry and parallel collimator with the resolution of 0.0001 degree. XRD beam was from the Cu source, Kα1 line λ=1.5418 Å, 45 kV, 40 mA and the angles used were from 20° to 80° with a step size of 0.05° and step time of 100 s.

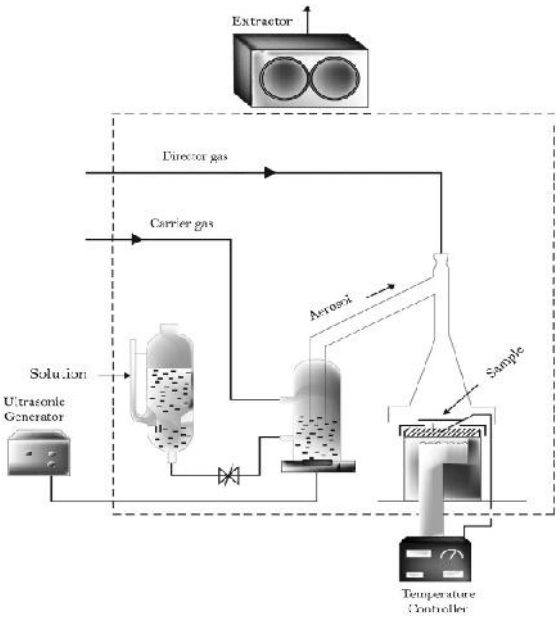


**Figure 1.** Schematic diagram of the experimental setup used for the deposition of the ZnO:Ag films by the ultrasonic spray pyrolysis method.

## EXPERIMENTAL RESULTS AND DISCUSSION

SEM images of the typical ZnO:Ag NCs obtained at the deposition times of 3 and 10 min for two substrate temperatures are presented in figure 2. It is clear that the ZnO NCs have the hexagonal cross section and the road orientation along the c axis. The cross section of ZnO NCs increases with the temperature and durations of the UPS process (Table 1).

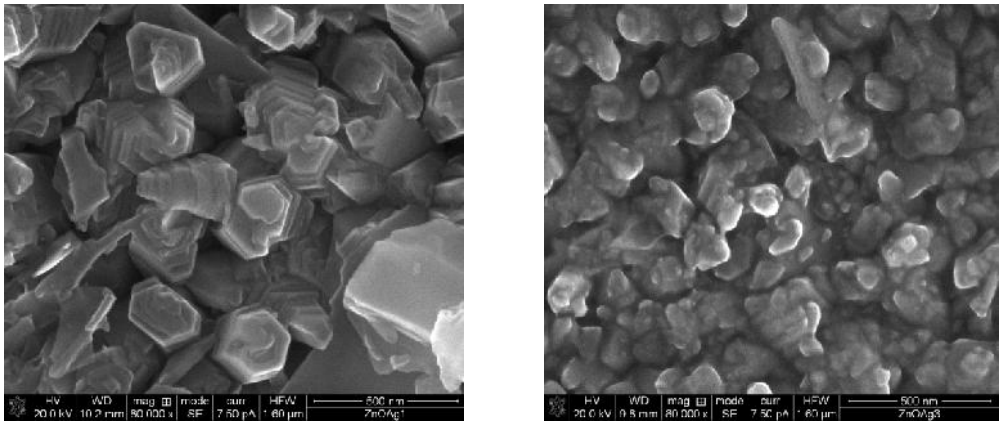

a) b)

**Figure 2.** SEM images of the samples prepared at the substrate temperatures 400$^{o}$C (a, b) and the durations of 10 (a) and 3min (b).

X-ray diffraction patterns of ZnO:Ag NCs obtained on the substrate with the temperature of 400$^{o}$C and different deposition durations are shown in Fig. 3. At low deposition time (3min) the ZnO films showed an amorphous phase mainly with very small (100), (002) and (10 1) peaks. These peaks are the evidence of starting the conversion of an amorphous phase into a polycrystalline one. It was observed that with increasing the deposition duration from 3min to 10min, a set of new peaks appears, which correspond to the X- ray diffraction from the (100),

(002), (101), (102), (110), (103) and (200) crystal planes (the angles 2θ equal to 31.770, 34.422, 36.253, 47.540, 56.604, 62.865 and 68.709 degrees), respectively, in the wurzite ZnO crystal structure with the hexagonal lattice parameters of a=3.2498A and c=5.2066A [13]. The (0 0 2) reflection peak is intense and sharper, as compared to the other peaks, indicating a preferential c-axis orientation of ZnO:Ag NCs.

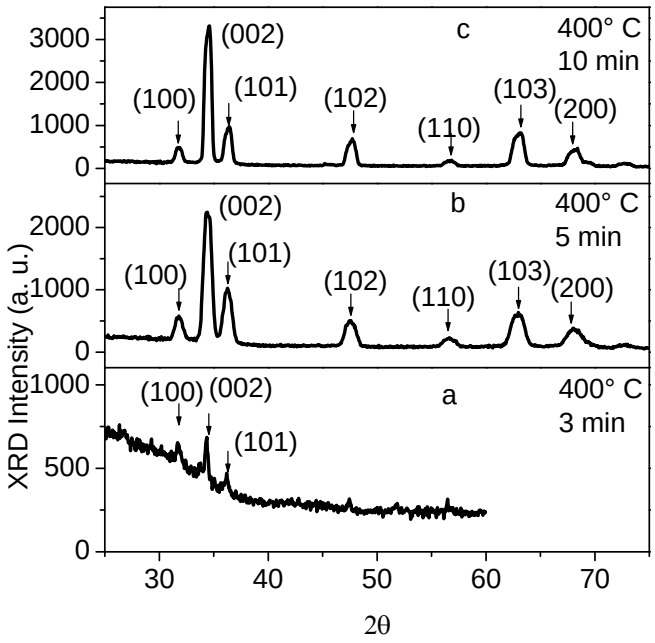


**Figure 3.** XRD diagrams of studied samples prepared on the substrate with T = 400° C at the deposition times of 3 (a), 5 (b) and 10 (c) min.

PL spectra of ZnO:Ag NCs are shown in figure 4. It is clear that the PL spectra are complex and can be represented as a superposition of elementary PL bands with the peaks in the spectral ranges: 3.14 eV (I), 2.00-2.70 eV (II) and 1.57 eV (III) (Fig.4). It is known that the UV-visible PL bands in ZnO owing to the near-band-edge (NBE) or exciton (I) and defect-related (II) recombination [14-17]. With increasing the substrate temperature the NBE related PL bands in the range I enlarged mainly, in comparison with the defect related (II) PL bands (Fig.4). At the same time the PL peak position of defect related PL bands shifts into the high energy (to 2.5 eV). With increasing the USP durations the intensity of defect related PL bands (II) raises mainly in comparison with those of NBE PL bands (Fig.4).

A great variety of luminescence bands in the UV and visible spectral ranges have been detected in the ZnO crystals [14]. The origin of these emissions has not been conclusively established. The NBE emission at 3.0-3.37 eV is attributed to the free (FE) or bound (BE) excitons, their LO phonon replicas, such as FE-1LO or FE-2LO, to optical transition between the free to bound states, such as the shallow donor and valence band, or to donor-acceptor pairs [14].

The blue PL band with the peak at 2.75-2.80 eV is attributed to Cu related defects [18], to Zn interstitials [19] or to donor-acceptor pairs including the shallow donor and oxygen vacancy [20]. The defect related green PL band in the spectral range 2.20-2.50 eV in ZnO is assigned ordinary to oxygen vacancies [19], Cu impurities [18] or surface defects [21]. The orange PL band with the peak at 2.02-2.10 eV was attributed earlier to oxygen interstitial atoms (2.02 eV) [22] or to the hydroxyl group (2.10eV) [23]. Taking into account that the PL intensity of

2.25 eV PL band increased with raising the USP duration the assumption that the corresponding defects are related to oxygen vacancies looks very reliable.

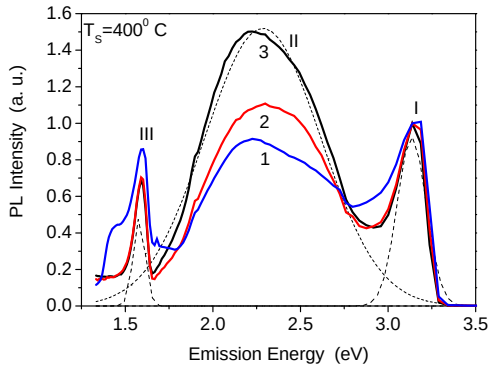


**Figure 4a.***(color online)* PL spectra of samples prepared on the substrate with T = 400° C at the deposition times: 1-3 min, 2-5min, 3-10min.

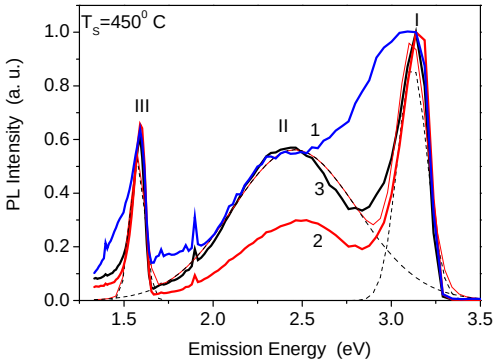


**Figure 4b**. *(color online)* PL spectra of samples prepared on the substrate with T = 450° C at the deposition times: 1-3 min, 2-5min, 3-10min.

Studied ZnO films were doped by Ag and, therefore, have the acceptor type defects, $Ag_{Zn}$, which were formed when the Ag atoms substitute of Zn atoms in the ZnO crystal lattice. Emission of the acceptor type defects in ZnO has been studied intensively during the last two decades as well. Note, the broad PL bands with the peaks at 3.238 and 3.315 eV at 4.3K earlier have been observed in acceptor N doped MBE ZnO crystals [24]. These peaks were assigned to acceptor ($N_o$) bound exciton (3.315 eV), to donor-acceptor pair emission, involving $N_o$ acceptor, or to the LO-phonon replica (3.238eV) of the donor BE line [24]. With temperature increasing the NBE intensity of acceptor bound exciton fallen down due to the dissociation of bound excitons and the FE band with it's LO replicas dominates in the Pl spectrum. Thus in our case the 3.14 eV PL band in the room temperature PL spectrum can be attributed to the LO phonon replica of FE emission. Note that the variation of PL intensity of the 1.57 eV PL band correlate with the intensity variation of the 3.14 eV PL band that permits to assign of the 1.57 eV PL band to the second-order diffraction peak of 3.14 eV PL band.

## CONCLUSIONS

ZnO:Ag NCs with hexagonal structures have been successfully synthesized by the USP method. With increasing the substrate temperature at USP up to 450$^o$C the PL intensity of NBE related emission bands has enlarged. The study has revealed three types of PL bands that in the room temperature PL spectrum related to the LO replicas of FE and its second-order diffraction peak, as well as the defect-related PL band, apparently, connected with oxygen vacancies. The PL band related to the LO phonon replicas of free exciton and its second-order diffraction in the PL spectra at room temperature testify on the high quality of the ZnO:Ag films prepared by USP.

## REFERENCES

1. Pearton, S.J., Norton, D.P., Ip, K., Heo, Y.W., Steiner, T. Prog. Mater. Sci. **50**, 293 (2005).
2. Koch, M.H., Timbrel1,P.Y., Lamb, R.N. Semicond. Sci. Technol. **10**, 1523 (1995).

3. Vanheusden,K., Seager,C.H., Wareen, W.L., Tallant, D.R., Caruso, J., Hampden-Smith, M.J., Kodas,T.T.,Lumin.J. **75** , 11 (1997)
4. Yang,Z.K., Yu,P., Wong, G.L., Kawasaki, M., Ohtomo, A., Koinuma, H., Segawa, Y. Solid State Commun. **103**, 459 (1997).
5. Alvi,N.H., Usman Ali, S.M., Hussain, S., Nur, O. and Willander,M. Scripta Materialia **64**, 697 (2011).
6. Huang,M.H., Mao, S., Feick, H. Science **292,** 1897 (2001).
7. Scheer,R., Walter, T., Schock, H.W., Fearheiley, M.L., Lewerenz, H.J. Appl. Phys. Lett. **63,** 3294 (1993).
8. Chen,Y., Baghall, D.M., Koh, H., Park, K., Hiraga, K., Zhu, Z., Yao, J. T.Appl. Phys**. 84,** 3912 (1998).
9. Li,Y.B., Bando, Y., Golberg, D. Appl. Phys. Lett. **84** , 3603 (2004).
10. Ding,J., McAvoy, T.J., Cavicchi, R.E., Semancik, S.Sens. Actuat. B **77** , 597 (2001).
11. Dybic,M., Ostapenko, S., Torchynska, T.V., Velazquez Lozada, E. Appl. Phys. Lett**. 84** (25), 5165 (2004)
12. Torchynska,T. V., Diaz Cano, A.I., Dybic, M., Ostapenko, S., Mynbaeva, M. Physica B, Condensed Matter, **376-377**, 367 (2006)
13. PDF2 XRD database, card no. 36-1451.
14. Djuris,A. B., Ng, A.M.C., Chen, X.Y. Progress in Quantum Electronics 34. 191-259 (2010).
15. Korsunskaya,N.E., Markevich,I.V., Torchinskaya T.V.,and Sheinkman, M.K. J. Phys. Chem. Solid. **43,** 475-479 (1982).
16. Korsunskaya,N.E., Markevich,I.V., Torchinskaya T.V., andSheinkman, M.K. J. Phys. C. Solid St.Phys. **13**, 2975 -2982 (1980).
17. Korsunskaya,N.E., Markevich, I.V., Torchinskaya T.V., and Sheinkman,M.K. phys. stat. sol (a), **60**, 565 -572 (1980).
18. Reshchikova,M.A., Morkoc, H., Nemeth, B., Nause, J., Xie, J., Hertog, B., Osinsky, A. Physica B, Condensed Matter, 401–402, 358–361 (2007).
19. Patra,M.K., Manzoor, K., Manoth, M., Vadera, S.P., Kumar, N., Lumin, J. 128 (2) 267–272 (2008).
20. Zhang,D.H., Xue, Z.Y., Wang, Q.P. J. Phys. D: Appl. Phys. 35 (21) 2837–2840 (2002).
21. Djurišic,A.B., Choy, W.C.H., Roy, V.A.L., Leung, Y.H., Kwong, C.Y., Cheah, K.W., Gundu Rao, T.K., Chan, W.K., Lui, C. H.F. Surya, Adv. Funct. Mater. 14 856-864 (2004).
22. Liu,X., Wu, X., Cao, H., Chang, R.P.H. J. Appl. Phys. 95 (6) 3141–3147 (2004).
23. Qiu,J., Li, X., He, W., Park, S.-J., Kim, H.-K., Hwang, Y.-H., Lee, J.-H., Kim, Y.-D. Nanotechnology 20 155603 (2009).
24. Look,D.C., Reynolds, D.C., Litton, C.W., Jones, R.L.,Eason, D.B, Cantwell, G. Appl. Phys. Lett. **81**,1830 (2002).